Developmental Expression of Fibrillin Genes Suggests Heterogeneity of Extracellular Microfibrils

Hui Zhang, Wei Hu, and Francesco Ramirez

Brookdale Center for Molecular Biology, Mount Sinai School of Medicine, New York 10029

Abstract. Extracellular microfibrils, alone or in association with elastin, confer critical biomechanical properties on a variety of connective tissues. Little is known about the composition of the microfibrils or the factors responsible for their spatial organization into tissue-specific macroaggregates. Recent work has revealed the existence of two structurally related microfibrillar components, termed fibrillin-1 and fibrillin-2. The functional relationships between these glycoproteins and between them and other components of the microfibrils and elastic fibers are obscure. As a first step toward elucidating these important points, we compared the expression pattern of the fibrillin genes during mammalian embryogenesis. The results revealed that the two genes are differentially expressed, in terms of both developmental stages and tissue distribution. In the majority of cases, fibrillin-2 transcripts appear earlier and accumulate for a shorter period of time than fibrillin-1 transcripts. Synthesis of fibrillin-1 correlates with late morphogenesis and the appearance of well-defined organ structures; fibrillin-2 synthesis, on the other hand, coincides with early morphogenesis and, in particular, with the beginning of elastogenesis. The findings lend indirect support to our original hypothesis stating that fibrillins contribute to the compositional and functional heterogeneity of the microfibrils. The available evidence is also consistent with the notion that the fibrillins might have distinct, but related roles in microfibril physiology. Accordingly, we propose that fibrillin-1 provides mostly force-bearing structural support, whereas fibrillin-2 predominantly regulates the early process of elastic fiber assembly.

ELASTIC fibers are extracellular aggregates responsible for most of the elastic properties of the connective tissues (see reviews by Cleary and Gibson, 1983; Ramirez et al., 1993; Rosenbloom et al., 1993; Mecham and Davis, 1994). Elastic fibers can vary in length, thickness, and spatial arrangement, depending on the strength and direction of the forces normally experienced by individual tissues. Elastic fibers can therefore form a variety of tissue-specific macroaggregates, such as concentric lamellae in vessels, highly branched networks in cartilage, and parallel thin fibers in ligaments. Regardless of the individual appearance, all elastic fibers are characterized by an amorphous core of cross-linked elastin surrounded by a peripheral mantle of tubular microfibrils (Cleary and Gibson, 1983; Mecham and Davis, 1994). Virtually nothing is known about the steps leading to the assembly of an elastic fiber, or the physical relationships among its structural constituents. Like other complex macroaggregates, tri-dimensional organization of elastic fibers is likely to represent the end-product of a hierarchical process governed by structural and cellular factors. The spatiotemporal diversification of the microfibrils might conceivably be one of the critical determinants in the assembly of tissue-specific aggregates. This prediction is consistent with the diversified roles that the microfibrils are believed to play. These roles include being the scaffold that guides elastin deposition and fiber assembly; connecting different matrix components; preventing excessive fiber stretching; and devoid of elastin, holding organ structures into place (Rosenbloom et al., 1993; Mecham and Davis, 1994).

The biochemical composition of different microfibrils has yet to be determined. At least three distinct groups of glycoproteins are believed to contribute to microfibril formation: fibrillin, microfibril-associated glycoprotein, and associated microfibril protein (Sakai et al., 1986; Gibson et al., 1991; Horrigan et al., 1992). The importance of fibrillin has been recently strengthened by the discovery that mutations in this protein lead to the pleiotropic manifestations of Marfan syndrome (Dietz et al., 1991). The seminal work of Sakai et al. (1986, 1991) led to the original identification of this 350-kD extracellular glycoprotein (now known as fibrillin-1 or fib-1) using antibodies against a microfibrillar extract from term placenta. The biochemical characterization of fib-1 laid the ground for the subsequent cloning of the corresponding human gene (*FBN1*) (Maslen et al., 1991; Lee et al., 1991; Corson et al., 1993; Pereira et al., 1993). Contrary to previous

Address all correspondence to F. Ramirez, Brookdale Center for Molecular Biology, Mt. Sinai School of Medicine, One Gustave L. Levy Place, New York, NY 10029. Tel.: (212) 241-1757. Fax: (212) 860-9279.

belief, the cloning work revealed fibrillin heterogeneity, for it identified a structurally related but genetically distinct product, subsequently called fibrillin-2 or fib-2 (Lee et al., 1991; Zhang et al., 1994). Furthermore, the fib-2 locus (*FBN2*) was genetically linked to congenital contractural arachondactyly, a dominant disorder with skeletal manifestations somewhat resembling those of Marfan syndrome (Lee et al., 1991). The structural similarities of the proteins and the clinical overlaps between the disorders led us to hypothesize that the fibrillins may have distinct, but related roles in microfibril physiology (Lee et al., 1991). Subsequent immunohistochemical work provided indirect support for this notion in that it showed preferential accumulation of fib-2 in elastic fiber-rich matrices of the human embryo (Zhang et al., 1994). The analysis was, however, limited to two tissues and a single developmental stage.

Accordingly, the current study was designed to confirm and extend that preliminary survey by performing a comparative analysis of the expression of the two fibrillin genes during mouse embryogenesis. The results document the differential expression of the two genes during development and in a large variety of tissues, thus implying that morphologically identical microfibrils are actually heterogeneous in composition. This conclusion indirectly corroborates the hypothesized functional diversity of the fibrillin proteins.

Materials and Methods

Cloning Experiments

The mouse cDNA library used in this study (a kind gift of Dr. T. Lufkin, Mt. Sinai School of Medicine) was engineered in the λZAPII vector (Stratagene, La Jolla, CA) using RNA purified from embryos at 10.5 d postcoitum (d.p.c.).[1] The cDNA library was screened with human fib-2 coding probes (Zhang et al., 1994) at 42°C in 50% formamide, 5× SSC (1× SSC: 0.15 M NaCl, 15 mM sodium citrate, pH 7.0), 1× Denhardt's solution (1% Ficoll, 1% polyvinylpyrrolidone, 1% BSA), 50 μg/ml sheared salmon sperm DNA (Sambrook et al., 1989). After hybridization, filters were washed under gradually increasing stringency up to 0.5× SSC at 50°C (Sambrook et al., 1989). Positive cDNA inserts were excised from the phage, recircularized into the Bluescript vector (Stratagene), and sequenced using the dideoxynucleotide chain termination method on denatured double-stranded DNA (Zagurski et al., 1986). When appropriate, additional cDNA sequences were derived from amplification of reverse-transcribed mRNA using the PCR technique (Kawasaki and Wang, 1989). Sequences were analyzed using the computer program MacVector (International BioTechnologies Inc., New Haven, CT).

Immunohistochemistry

Characterization of the anti-fibrillin antibodies used for immunohistochemistry has been described by Zhang et al. (1994). Tissue samples from a 17-d-old rat embryo were paraffin embedded and cut into consecutive sections ~8–10-μm thick (Zhang et al., 1994). They were dewaxed with xylene and rehydrated with a graded series of ethanol immersions. Intrinsic peroxidase activity was blocked by immersion in a methanol solution containing 3% hydrogen perioxidase for 10 min, followed by blocking with 10% goat serum for 2 h at room temperature. Primary antibodies (1:100 dilution) were incubated on the slides overnight at 4°C. After several PBS washes, biotinylated goat anti-rabbit IgG was added to the slides for 1 h, and streptavidin-peroxidase and DAB chromogen supplied with the Vectastain ABC kit (Vector Laboratories Inc., Burlingame, CA) were used following the manufacturer's recommendations. Stainings were viewed and photographed with a Zeiss Axiophot microscope (C. Zeiss Inc., Thornwood, NY).

1. *Abbreviation used in this paper*: d.p.c., days postcoitum.

In Situ Hybridization

Mouse embryos from different developmental stages were dissected and quickly fixed in fresh 4% paraformaldehyde in PBS at 4°C overnight (Andrikopoulos et al., 1992). Embryos were dehydrated by a series of immersions in graded ethanol, cleared with two changes of xylene, and embedded in Paraplast Plus (Fisher Scientific, Springfield, NJ) at 60°C for 2 h with three changes of wax. Embryo samples were then serially cut into 6–8-μm sections spread onto Superfrost/Plus slides (Fisher Scientific). Before hybridization, slides were rehydrated and treated for 30 min at 37°C with 1 μg/ml proteinase K in 0.1 M Tris-HCl, pH 8.0, 50 mM EDTA. The same buffer without the enzyme was used to wash the slides, which were incubated at room temperature for 10 min in 0.1 M glycine, pH 8.0, 0.2 M Tris-HCl, pH 8.0, and were finally acetylated for 10 min at room temperature by treatment with 0.25% acetic anhydride in 0.1 M triethanolamine. This step was followed by rinsing with 2× SSC and dehydration with graded ethanol. The fibrillin-1 and -2 probes used in this study are of similar size (880 and 840 bp), and both cover 3′ noncoding segments of the respective mRNAs (Fig. 1; Yin et al., 1995). About 1 μg of each plasmid, linearized with the appropriate restriction enzyme, was transcribed with T7 polymerase in the presence of [^{35}S]UTP as previously described (Su et al., 1991). After removal of the DNA template, probes were hydrolyzed to an average size of 100–150 nucleotides and cleared of free nucleotides through a G50 Sepharose column. Hybridizations were performed in 50% formamide, 0.3 M NaCl, 20 mM sodium acetate, pH 5.0, 5 mM EDTA, 10% dextran sulfate, 1× Denhardt's solution, 500 μg/ml yeast tRNA, 0.1 M DTT. About 4×10^4 cpm of probe was added to 1 μl of the hybridization mix, and ~5 μl/cm^2 of such mix was added to the tissue sections, which were then covered with clean coverslips. After a 16-h incubation at 50°C, slides were washed with four changes of 4× SSC, 10 mM DTT at 50°C for 2 h and with two changes of 50% formamide, 2× SSC, 10 mM DTT at 50°C for 2 h. After equilibration in TNE buffer (0.5 M NaCl, 10 mM Tris-HCl, pH 8, 1 mM EDTA), slides were treated with 20 μg/ml RNase A, 1 U/ml RNase T1 for 40 min at 37°C. After several washes in decreasing salt concentrations (down to 0.1× SSC in 10 mM β-mercaptoethanol) and dehydration, slides were dipped into photographic emulsion (NBT-2; Eastman Kodak Co., Rochester, NY) at 42°C in the dark. After development and hematoxylin counterstraining, slides were dehydrated, mounted, and photographed under bright- and dark-field illumination.

Results

Cloning of the Mouse Fibrillin-2 cDNA

Overlapping cDNAs coding for the human fib-2 protein were initially used to screen a mouse embryonic library under cross-hybridizing conditions (Zhang et al., 1994). This led to the isolation of several positive clones that were found to contain most of the coding sequence of the mouse fib-2 (*fbn2*) gene (Fig. 1). Incidentally, the sequence of one of the cDNAs (clone m7 in Fig. 1) is identical to that of the genomic clone that was previously used to locate the *fbn2* gene to band 18D-E1 of mouse chromosome 18 (Li et al., 1993). Gaps between clones m2 and m3 and between m3 and m8 were subsequently resolved by sequencing two reverse transcriptase PCR products (clones P-274 and P-256 in Fig. 1). The cloning effort ultimately resulted in the isolation of eight cDNAs covering the whole 8721-nucleotide coding sequence of the *fbn2* gene, in addition to an 880-bp clone (mF) that contains only 3′ noncoding sequence (Figs. 1 and 2). Pairwise comparison with the human sequence identified a 7-amino acid insertion and two single-amino acid deletions in the human chain (Fig. 2); as a result, the mouse polypeptide is slightly shorter than the human. The analysis also revealed two sequencing errors in the human gene: between amino acids 192 and 194 (GPNR instead of A-QP) and between amino acids 2908 and 2918 (QIQLY instead of QKHLKSQGLIK). Location of the changes is based on the

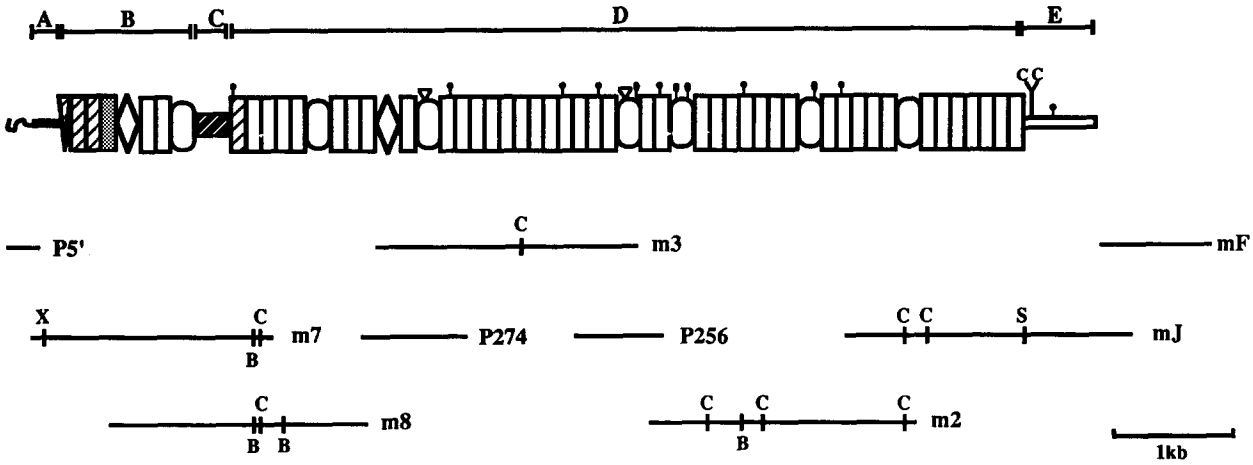

Figure 1. Restriction map of the mouse cDNA clones coding for the fib-2 protein (shown schematically above the clones). The structural elements of the protein are designated by the same symbols and divided into the same regions as the human protein described by Zhang et al. (1994). Letters in the cDNAs indicate the following restriction enzymes: *B*, BamHI; *C*, ClaI; *S*, SphI; and *X*, XbaI.

previous amino acid numbering of human fib-2 (Zhang et al., 1994).

The protein encoded by *fbn2* exhibits 97% identity with the human counterpart and 76% with the mouse *fbn1* gene product (Zhang et al., 1994; Yin et al., 1995). It contains the same structural features originally noted in the human proteins (Maslen et al., 1991; Corson et al., 1993; Pereira et al., 1993; Zhang et al., 1994). They include the total number of residues in individual cysteine-rich repeats and the relative spacing between the cysteinyl residues of each repeat; the location and number of the putative glycosylation sites and cell attachment sequences; and the polylysine stretches and cysteinyl residues of the COOH-terminal region (Fig. 2). Of particular interest is the phylogenetic conservation of the most divergent sequence of the two fibrillin proteins, notably the short glycine-rich segment located near the NH_2 terminus of fib-2 (region C in Fig. 1) (Zhang et al., 1994). It has been previously shown that nearly half of the corresponding sequence of fib-1 is instead made of proline residues (Pereira et al., 1993; Corson et al., 1993).

Availability of cDNAs specific for the mouse fibrillin genes enabled us to select the most appropriate probe for the in situ hybridizations. In the case of *fbn2*, we chose the cDNA that contains only untranslated sequence with no homology with *fbn1* (clone mF in Fig. 1). We used the same criterion to select 3.5m, the 840-bp cDNA that includes part of the 3′ untranslated region of the mouse *fbn1* gene (Yin et al., 1995). Riboprobes from each clone were hybridized to serial sections of mouse embryos collected at 10.5, 13.5, and 16.5 d.p.c. Although not quantitative in nature, the experiments did enable us to compare the relative amounts of the two fibrillin mRNAs in each set of hybridizations. We in fact used identical amounts of comparably sized probes with similar specific activities, and we exposed the resulting autoradiograms for the same length of time. The value of this approach in detecting differences in steady-state mRNA levels can be readily appreciated by comparing the hybridization patterns in the same cephalic mesenchyme from 10.5-d.p.c. embryos (Fig. 3). Following is a more detailed description of the results obtained with different organ systems; these conclusively document differential expression of the fibrillins during embryogenesis.

Lungs

The developing lung is the best example illustrating the differential pattern of expression of the fibrillin genes. At 10.5 d.p.c., the lung buds are rapidly elongating, and the primary bronchi are present as small tubes (Kaufman, 1992). A strong *fbn2* signal was detected in the epithelial layer of the budding main bronchi along with a weaker and more diffuse signal in the primitive mesenchyme (Fig. 4 *A*). A similarly weak *fbn1* signal was seen in the mesenchymal cells of the lung, without additional expression in the bronchial epithelium (Fig. 4 *B*). As the lungs develop further, they subdivide into lobes, and secondary lobar bronchi and tertiary segmental bronchi continue to branch; by 13 d.p.c., branching of the segmental bronchi is the predominant feature of the forming lungs (Kaufman, 1992). Accumulation of the two fibrillin mRNAs was estimated to be comparable in the lung mesenchyme of 13-d.p.c. fetuses; in contrast, only *fbn2* transcripts were seen in the epithelium of the segmental bronchi (Fig. 4, *E* and *G*). Unlike the 10.5-d.p.c. lung samples, the epithelium of the main bronchi from 13.5-d.p.c. embryos showed very low amounts of *fbn2* transcripts (see Fig. 9 *A*). At stage 16.5 d.p.c., the lungs are still compact and terminal bronchi lined with cuboid cells begin to appear (Kaufman, 1992). The epithelial layer of the 16.5-d.p.c. segmental bronchi displayed little *fbn2* mRNA accumulation, whereas that of the sprouting terminal bronchi was now the most active sites (Fig. 4 *I*). Both fibrillin genes were instead active in the mesenchymal fibroblasts and smooth muscle cells (Fig. 4, *I* and *J*). Transcripts of the *fbn1* gene were clearly seen in the lung vasculature, but like earlier stages, not in the bronchial epithelium (Fig. 4 *J*).

To correlate mRNA accumulation with protein deposition, the in situ data were confirmed by immunohistochemical analysis of rat lung tissue from a developmental stage comparable to mouse 16.5 d.p.c. The choice of the rat tissue was deemed necessary in order to avoid the high background of

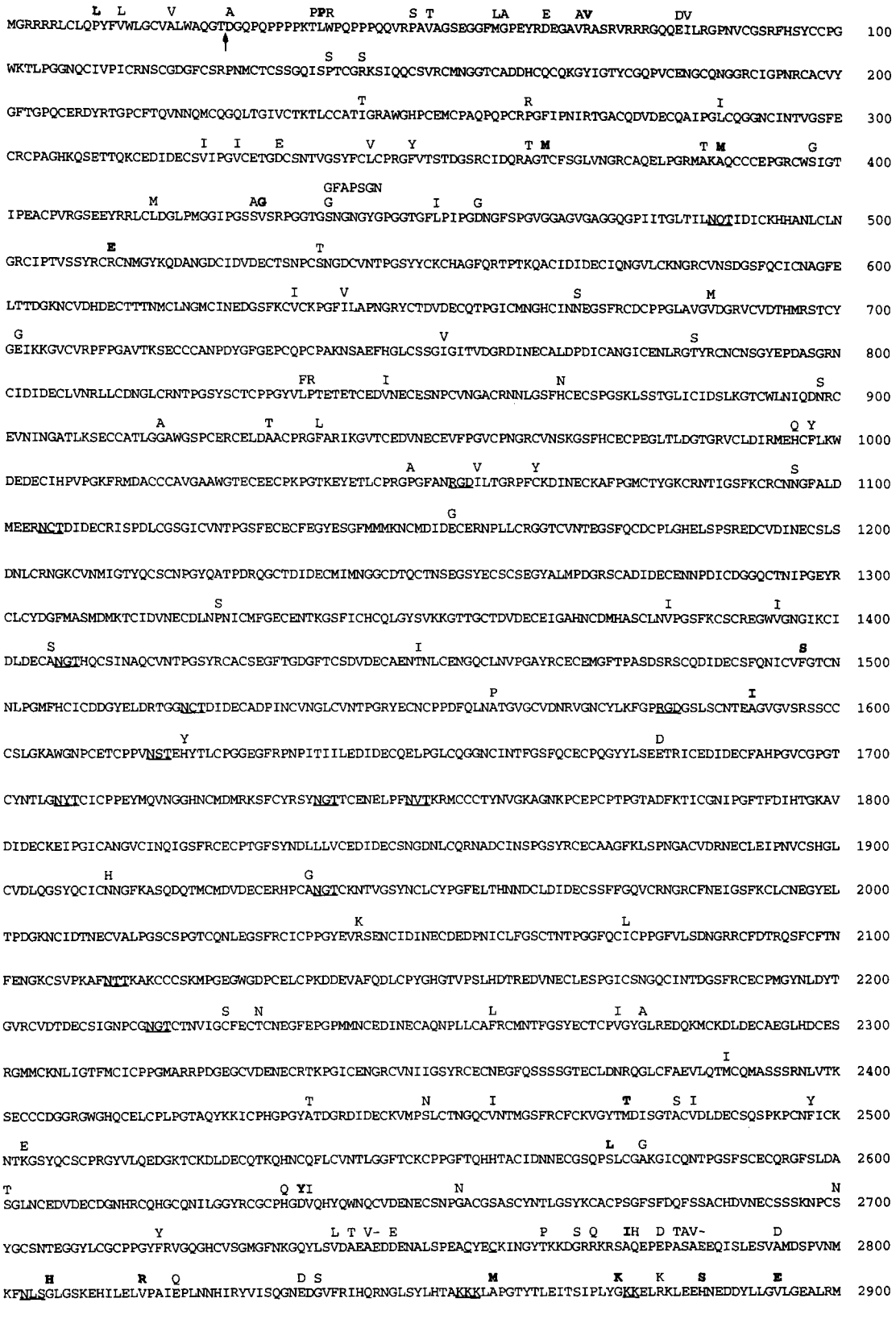

Figure 2. Amino acid sequence of the mouse fib-2 protein. Differences with the human polypeptide are shown above the sequence, with bold letters indicating nonconserved elements. Structural elements described in the text are underlined, and the putative signal peptidase sequence is highlighted by the arrow. As a result of the corrections discussed in the text, the length of the human product is different from that previously reported by Zhang et al. (1994). The complete nucleotide sequence is available from EMBL/Gene Bank/DDJB under accession number L39790.

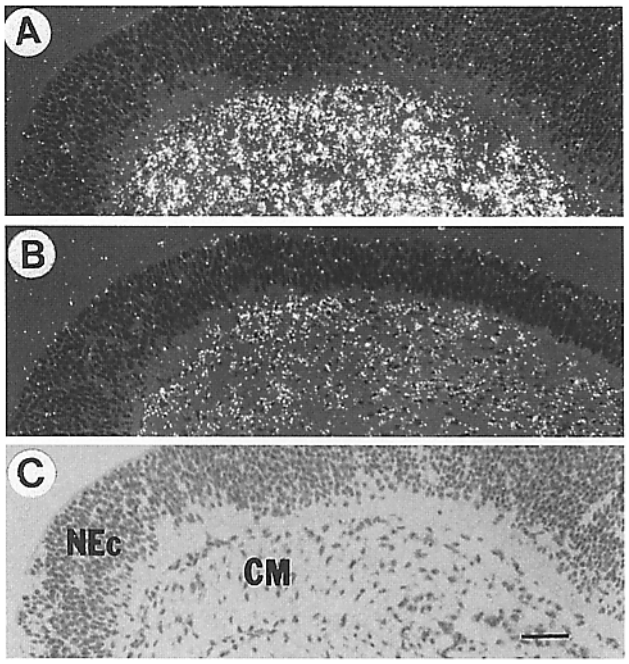

Figure 3. In situ hybridization of the 10.5-d.p.c. cephalic mesoderm (*CM*) to *fbn2* (*A*) and *fbnl* (*B*) probes. The neuroectodermal cells (*NEc*) of the brain serve as a negative internal control. Note that the accumulation of *fbn2* message in mesodermal cells is substantially greater than that of *fbnl*. Bar, 50 μm.

the rabbit anti-human antisera with mouse tissues. The immunohistochemical results yielded a pattern virtually identical to that of the in situ hybridizations. There was in fact homogeneous accumulation of the fib-1 and -2 proteins throughout the entire lung matrix, with preferential accumulation of the former protein around arteries and veins and of the latter in the area immediately surrounding the bronchial epithelium (Fig. 5). To summarize the data of the developing lung, the *fbn2* gene is selectively and transiently expressed in the epithelium of the forming bronchi; both fibrillins are coexpressed by the lung mesenchymal cells; and the *fbnl/fbn2* ratio progressively increases during the transition from the early to the late phase of lung morphogenesis.

Cartilage and Skeleton

Previous immunohistochemical staining of human auricular cartilage has shown very little deposition of fib-1 in the elastic core, where fib-2 is instead most abundant (Zhang et al., 1994). The in situ data confirmed the preponderance of *fbn2* gene expression in the elastic cartilage of the mouse larynx. At 13.5 d.p.c., the tissue destined to become epiglottis is separated by a discrete cleft from the rest of the larynx, which is still precartilaginous; by 15 d.p.c., the cartilaginous skeleton of the larynx and trachea becomes well delineated (Kaufman, 1992). Although poorly developed, the mesenchymal tissue of the 13.5-d.p.c. larynx contained substantial amounts of *fbn2* mRNA (Fig. 6, *A–C*). In 16.5-d.p.c. embryos, intense *fbn2* gene expression was observed in the elastic cartilage of the larynx, namely, the epiglottis and the cuneiform cartilage (Fig. 6 *D*). Expression of the *fbnl* gene in these structures was low and comparable to the levels in the surrounding tissue (Fig. 6 *E*). As in skeletal system (see the following discussion), coexpression of the fibrillins was seen mostly in the perichondrium of the laryngeal cartilages (Fig. 6, *D* and *E*).

The limbs of the 10.5-d.p.c. mouse embryo are composed mostly of primitive mesenchyme; cartilage begins to appear in the limbs at about 13 d.p.c.; ossification occurs in the skull and ribs around 15 d.p.c., but does not extend to the limbs until 16.5 d.p.c. (Kaufman, 1992). Fibrillin transcripts were identified in the developing mesenchyme of the limb bud as early as 10.5 d.p.c. (Fig. 7, *A–C*). Expression of *fbn2* was noted in the perichondrium of the developing long bones, ribs (flat bones), and vertebral bodies (short bones) with a characteristic pattern that highlighted the shape of the bone (Fig. 7, *D*, *G*, and *J*). Relatively less accumulation of *fbnl* transcripts was observed in the perichondrium, as well as in the cartilage itself, where very little *fbn2* expression was detectable (Fig. 7, *E*, *H*, and *K*). This pattern was even more evident in 16.5-d.p.c. embryos, in which *fbnl* transcripts were more abundant than in 13.5-d.p.c. fetuses (Fig. 7, *H* and *K*). At this stage of development, the *fbnl* signal was more evident in the hypertrophic and calcifying zones than other areas of the cartilage (Fig. 7 *K*). This last finding is consistent with previous immunohistochemical results indicating preferential accumulation of fib-1 around more differentiated chondrocytes (Zhang et al., 1994).

Both fibrillins were present in the cells of the ligaments and joints of 13.5- and 16.5-d.p.c. embryos, with an apparent prevalence of the *fbn2* over the *fbnl* transcript (Fig. 8). As it can be readily appreciated by comparing the relative intensity of the hybridizations in the 16.5-d.p.c. (Fig. 8, *M*) and 10.5-d.p.c. (Fig. 3, *CM*) embryo sections, the *fbnl/fbn2* ratio in the mesenchyme increased with a pattern similar to that observed in the developing lung (Fig. 4). The fibrocartilaginous intervertebral disc is another tissue that contains moderate amounts of elastic fibers. Expression of *fbn2* in this structure was intense and more localized to the peripheral annulus fibrosus; in contrast, a weaker and more diffuse *fbnl* signal was observed throughout the entire disc (Fig. 9). Together, the results seem to indicate that accumulation of *fbn2* transcripts in bone and cartilage peaks earlier than accumulation of *fbnl*; in turn, fib-1 appears to account for the largest proportion of the fibrillin produced by more mature tissues.

Cardiovascular System

At 10.5 d.p.c., the heart is still a single tube undergoing active morphogenesis of the aorticopulmonary spiral septum and the atrioventricular endocardial cushion. By 13.5 d.p.c., the ascending aorta and the pulmonary trunk are distinct vessels and the valves and septa of the heart are still primitive structures. Circulation starts around 14 d.p.c., when the communication between right and left ventricles is closed. Embryos at 16.5 d.p.c. have their heart and large vessels in the prenatal configuration (Kaufman, 1992).

Expression of the *fbnl* gene in the cardiovascular system was the only exception to the diphasic pattern seen in the other organ systems. Consistent with the recent report by Yin et al. (1995), substantial accumulation of *fbnl* transcripts was in fact detected as early as 10.5 d.p.c. in the aortic sac (Fig. 10, *C* and *E*). The signal remained intense throughout 13.5 and 16.5 d.p.c. in the full thickness of the aortic arch and pulmonary artery (Fig. 11 *B*). Expression of *fbn2* in these structures was always lower than that of *fbnl*, and the

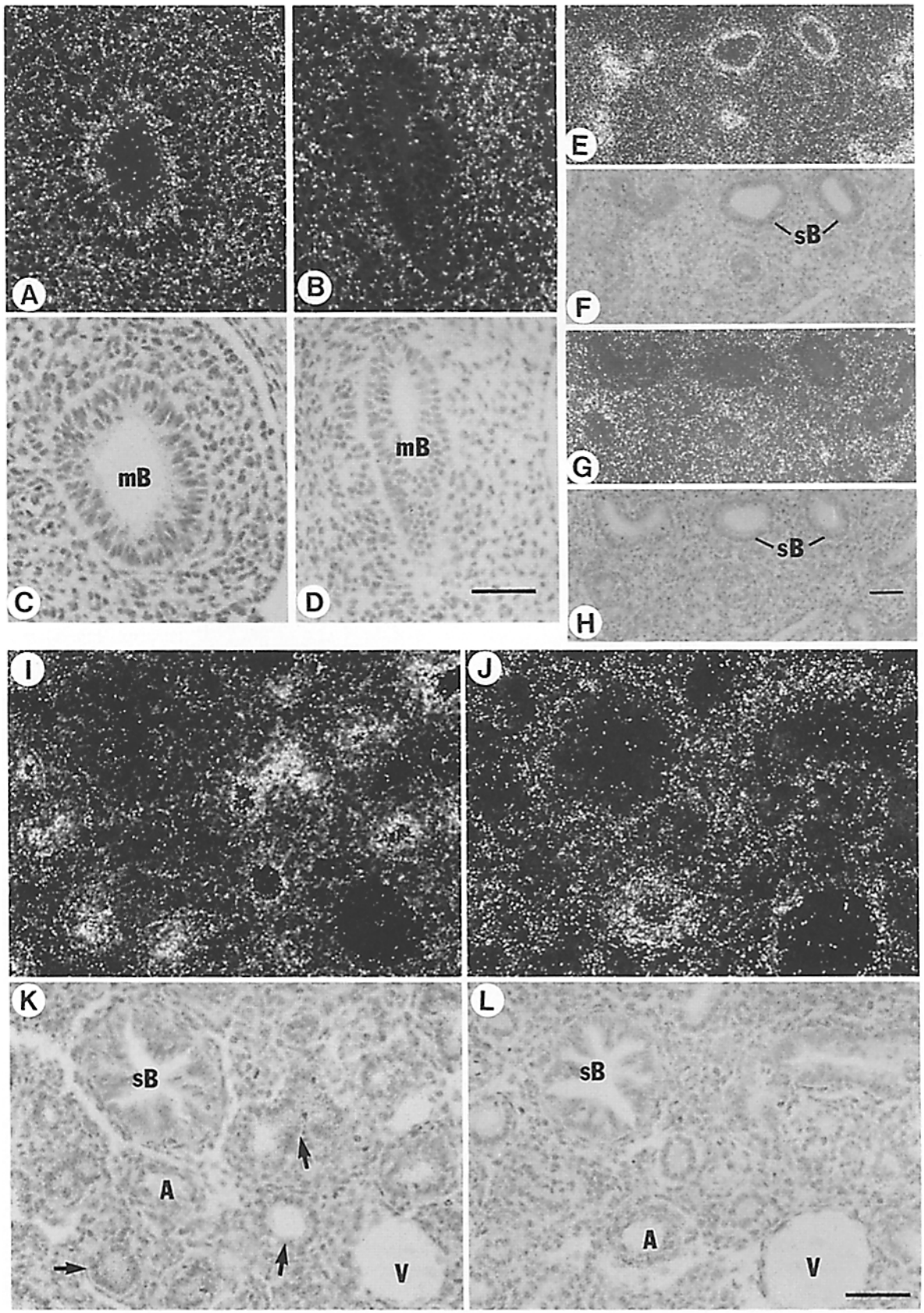

Figure 4. In situ hybridization of the lung bud at 10.5 d.p.c. (*A–D*) and the developing lungs at 13.5 d.p.c. (*E–H*) and 16.5 d.p.c. (*I–L*) to *fbn2* (*A*, *E*, and *I*) and *fbnl* (*B*, *G*, and *J*) probes. Expression of *fbn2* is in the epithelial cells of the main bronchi (*mB*), segmental bronchi (*sB*), and terminal bronchioles (*arrows*). Note the lack of *fbn2* signal in the segmental bronchi at 16.5 d.p.c. compared with earlier stages. Expression of *fbnl* at all stages is mostly in the lung parenchyma, arterioles (*A*), and venules (*V*). Bar, 50 μm.

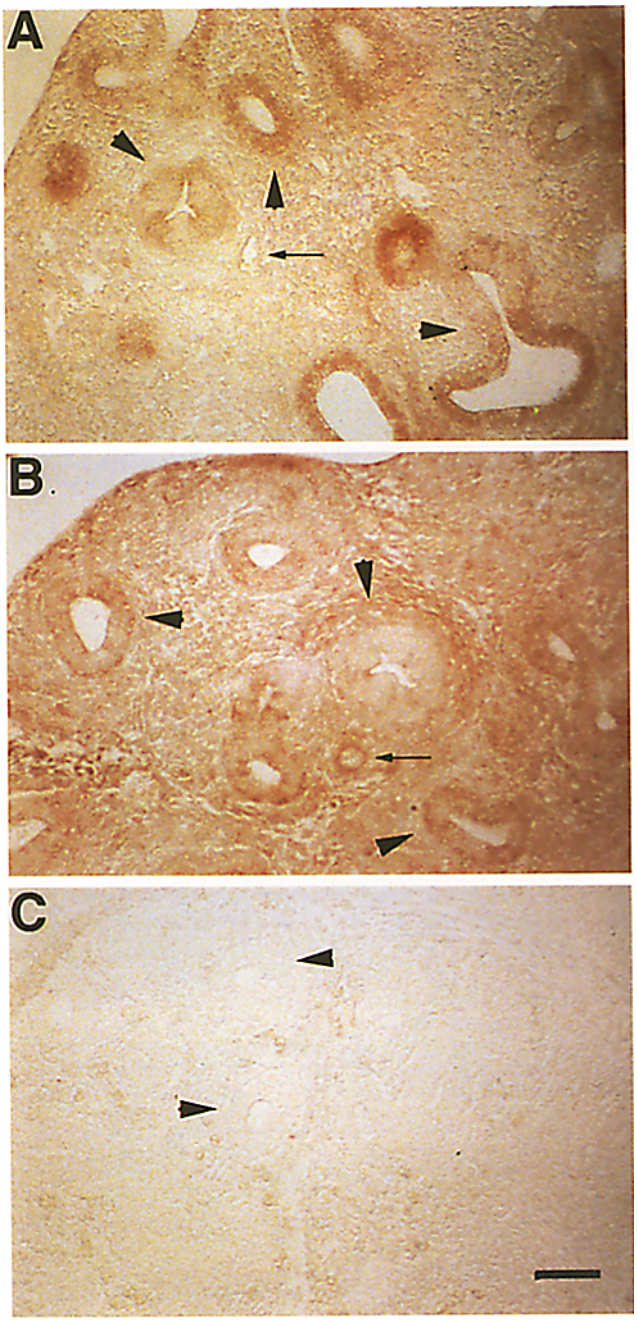

Figure 5. Immunohistochemical localization of fib-1 (*A*) and fib-2 (*B*) epitopes in rat fetal lung. Deposition of fib-2 is mostly around the newly formed bronchi (*arrowheads*). Arrows highlights the vessels of the developing lung. (*C*) Staining with preimmune sera. Bar, 100 μm.

difference gradually increased with development (Fig. 10 *A* and Fig. 11 *A*). The relatively low signal of *fbn2* might conceivably reflect the more localized expression in the media layer, particularly the outer part of the elastic and muscular arteries.

Transcripts from the *fbn2* gene were uniformly distributed in the myocardial cells of the heart; in contrast, *fbnl* expression was restricted mostly to the endothelial cells of the endocardium and the epithelial cells of the epicardium (Fig. 10 *A* and Fig. 11 *A*). Both genes were active in the endocardial cushion tissue associated with the wall of the atrioventricular canal and later responsible for the formation of the valves located between atrium and ventricle (Fig. 10, *A–D*). There was also noticeable accumulation of *fbnl* transcripts in the forming aorticopulmonary spiral septum (Fig. 10, *A–D*). Unlike *fbn2*, significant amounts of *fbnl* transcripts were detected in the arterioles of other tissues, such as the lung, kidney, and joints. In conclusion, the characteristics of fibrillin expression in the developing cardiovascular system are both common to and distinct from its expression in other organ systems; there is in fact the same differential tissue distribution of the two transcripts, but without the usual switch during morphogenesis of the relative ratio between the two species.

Other Tissues

In our survey we analyzed several other tissues and organs, with results virtually identical to those already described (data not shown). Briefly, *fbn2* transcripts were detected in the sclera of the eye as early as 13.5 d.p.c.; in the same organ, the *fbnl* signal was seen only at ~16.5 d.p.c. In the kidney transcription of the *fbnl* gene was observed mostly in the peritubular and extra-glomerular regions, whereas the activity of the *fbn2* gene was confined chiefly to the forming glomeruli. Subtle differences were also noted in the developing thymus and digestive system. In the former, both genes were expressed in the capsule, but only *fbn2* was active in the lobular septa. Likewise, the *fbnl* and *fbn2* genes were both transcribed by the submucosal cells of the intestine; additionally, *fbn2* was expressed in the cells of the lamina propria. The cells of the fibrous sheet of nervous tissues were another site of fibrillin coexpression. Relevant to the following discussion, a parallel survey of human samples showed consistently less fib-2 protein immunodetected in adult versus fetal skin, ligaments, and tendons.

Discussion

Work presented in this report extends further the characterization of the fibrillins by providing the first comparison of the pattern of gene expression during mammalian embryogenesis. The results add the spatiotemporal diversification of gene expression to the structural homologies and the overlapping pathologies of the fibrillins. Together, the data suggest that this small family of extracellular glycoproteins contributes to the biochemical diversity of seemingly identical microfibrils and, consequently, to the morphology and functional properties of the resulting macroaggregates. In addition, to clarify a few points, our analysis has also raised new questions regarding the composition of the microfibrils and the function of the fibrillins.

The fib-2 protein is produced mostly during embryogenesis by a wide variety of tissues and cells, including the mesenchyme, epithelium, chondrocytes, and vascular, skeletal, and cardiac muscle cells. This ubiquitous pattern of gene expression contrasts with the serendipitous discovery of the *fbn2* product during the cloning of the defective gene in Marfan syndrome (Lee et al., 1991). Data presented in this report strongly suggest that the age of the tissues used in previous biochemical and immunohistological studies might have been the principal reason for overlooking fibrillin het-

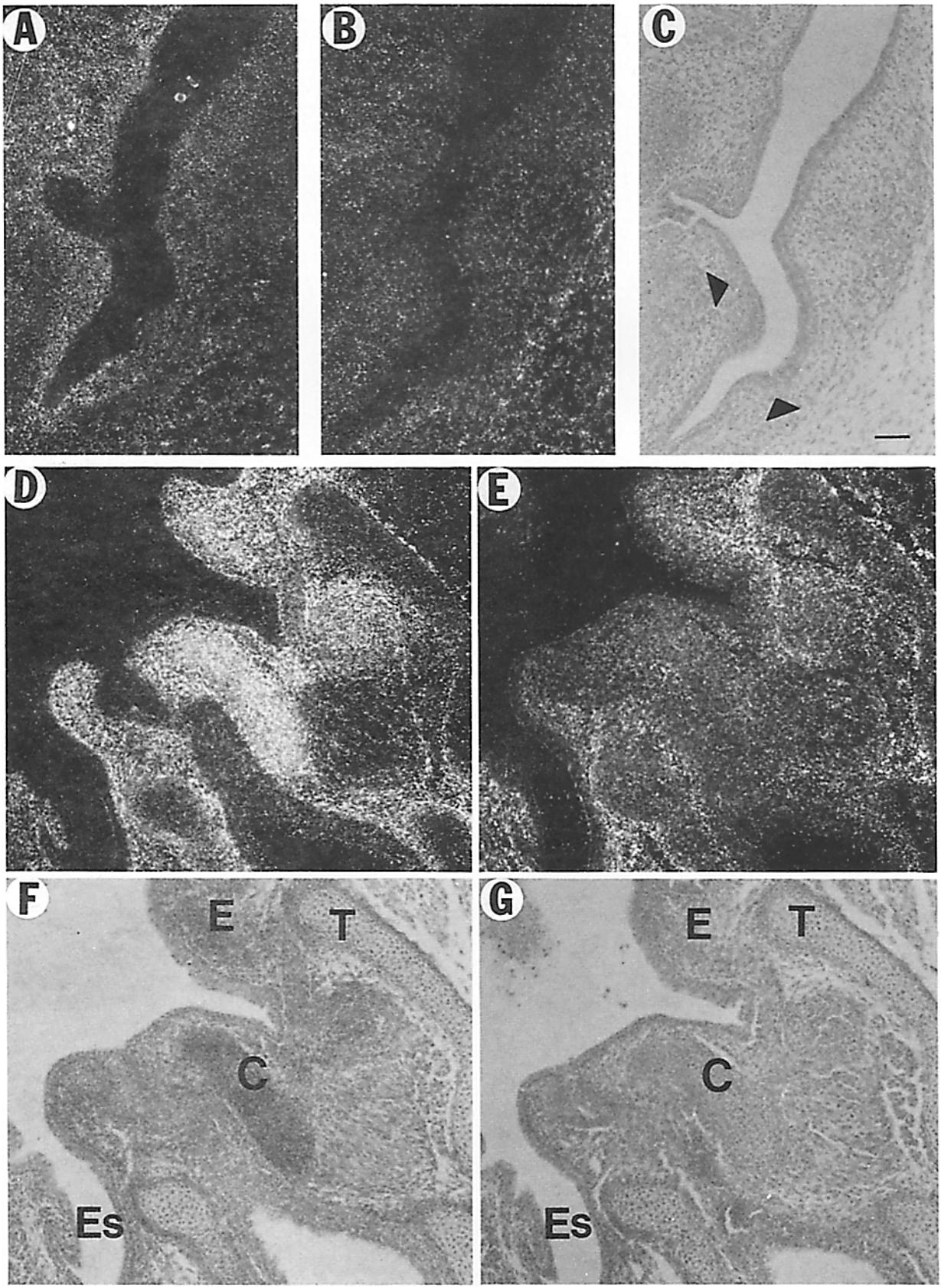

Figure 6. Expression of *fbn2* (*A* and *D*) and *fbnl* (*B* and *E*) in the laryngeal structures at 13.5 p.c. (*A–C*) and 16.5 d.p.c. (*D–G*). At 13.5 d.p.c., the mesenchymal cells (*arrowheads*) that later differentiate into the laryngeal structures have an enhanced accumulation of *fbn2* message. In the 16.5-d.p.c. mouse, the elastic cartilages of the larynx, epiglottis (*E*), and cuneiform cartilage (*C*) show high *fbn2* expression; in constrast, *fbnl* accumulation in these structures is not particularly great. Esophagus (*Es*) and thyroid (*T*) cartilages are also highlighted in the figure. Bar, 50 μm.

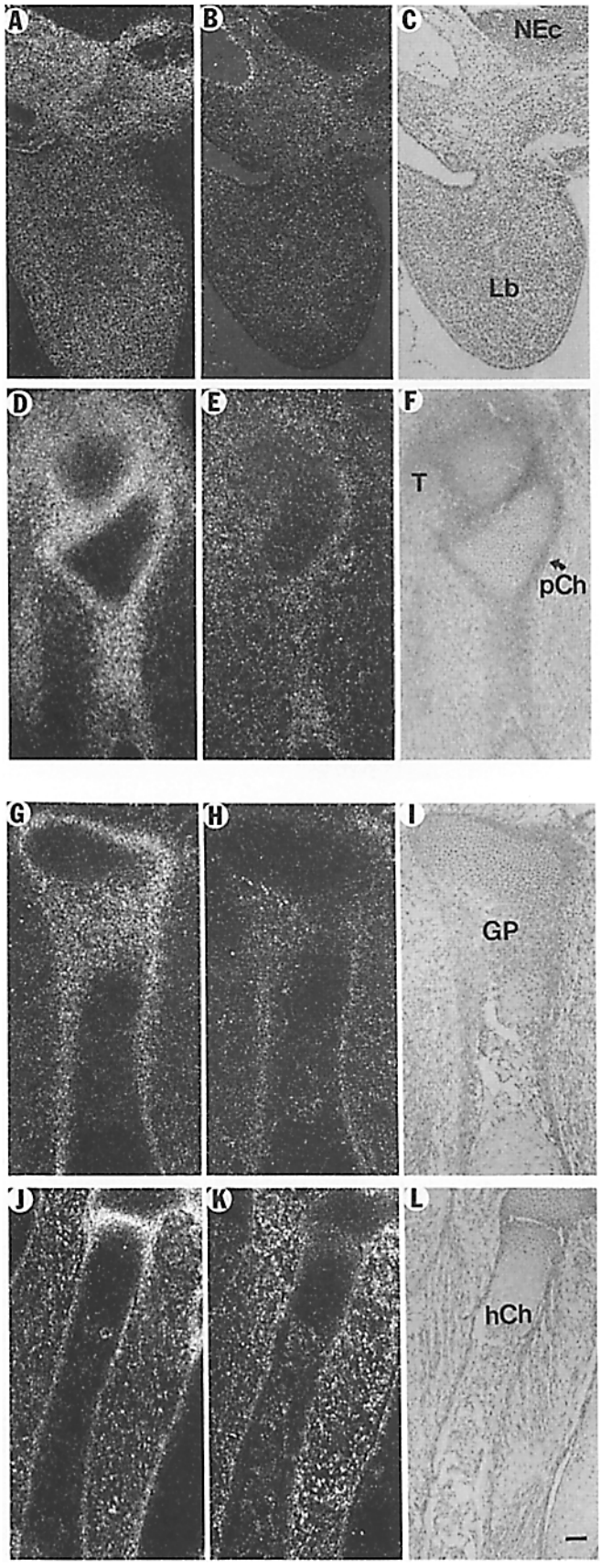

Figure 7. Expression of *fbn2* (*A*, *D*, *G*, and *J*) and *fbnl* (*B*, *E*, *H*, and *K*) in limb buds (*Lb*) at 10.5 d.p.c. (*A–C*), long bones at 13.5 d.p.c. (*D–F*) and 16.5 d.p.c. (*G–I*), and flat bones at 16.5 d.p.c. (*J–L*). Signals of the *fbn2* message are prominent in the cells of the perichondrium (*pCh*), growth plate (*GP*), and tendon (*T*). Expression of *fbnl* is widely distributed in the mesenchymal tissues with a slight increase in the perichondrium, growth plate, and hypertrophic chondrocytes (*hCh*). Both genes are silent in the neuroectoderm (*NEc*). Bar, 50 μm.

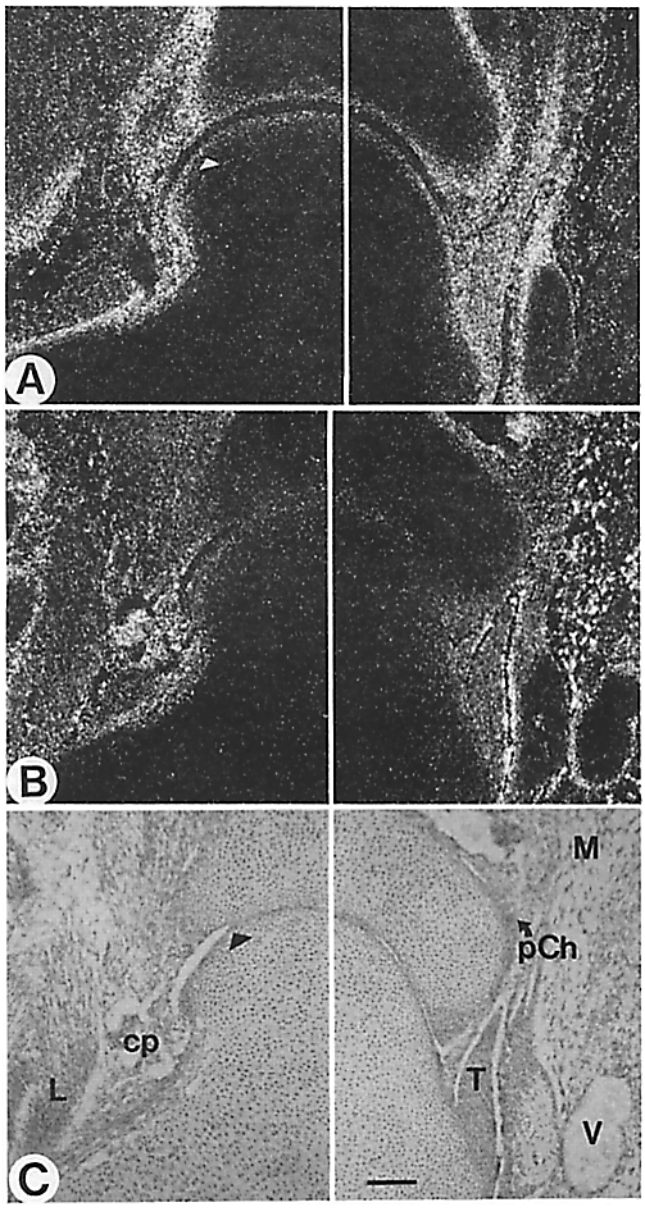

Figure 8. Expression of *fbn2* (*A*) and *fbnl* (*B*) in joints of the 16.5-d.p.c. mouse. Intense *fbn2* signals are noted in the cells of the perichondrium (*pCh*), ligament (*L*), tendon (*T*), and periphery of the cartilage (*arrowheads*). Expression of the *fbnl* gene is most noticeable in the capillaries (*cp*) around the joints, the venules (*V*), and the cells surrounding ligaments and tendons. In contrast with the 10.5-d.p.c. mouse (Fig. 3), intensity of the *fbnl* signal in mesenchymal cells (*M*) at this stage is higher than that of *fbn2*. Bar, 50 μm.

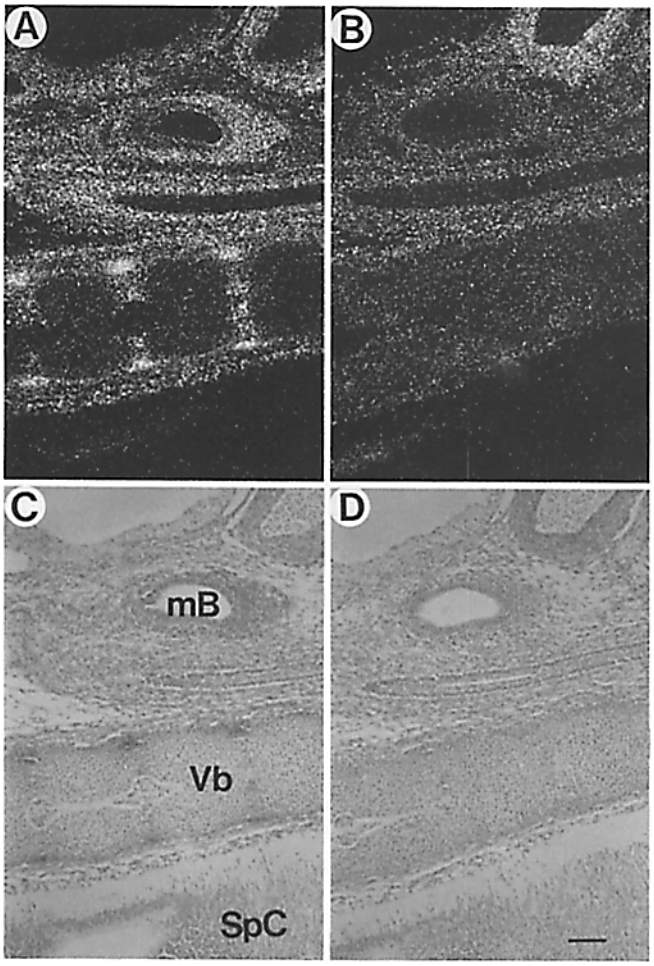

Figure 9. In situ hybridization of the main bronchi (*mB*), vertebral column (*Vb*), and the spinal cord (*SpC*) at 13.5 d.p.c. with *fbn2* (*A* and *C*) and *fbnl* (*B* and *D*). Bar, 50 μm.

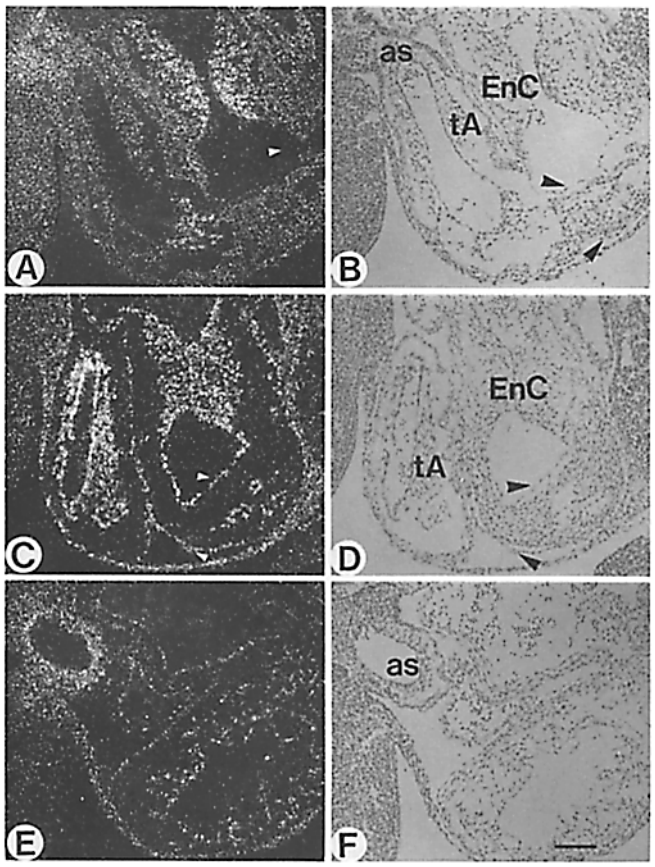

Figure 10. Expression of *fbn2* (*A* and *B*) and *fbnl* (*C–F*) in the 10.5-d.p.c. developing mouse heart. *fbn2* transcripts are seen in the myocardial cells, whereas *fbnl* transcripts are in the epi- and endocardial cells (*arrowheads*). The cells at the endocardial cushion (*EnC*) tissue produce both *fbn2* and *fbnl*. The truncus arteriosus region (*tA*), where the aorticopulmonary spiral septum is forming, shows strong *fbnl* expression. The wall of the aortic sac (*as*) expresses both fibrillins (*A* and *E*); note that only the edge of the aortic sac is on the section shown in *A*. Bar, 50 μm.

erogeneity. The anti-fibrillin antibodies used in the original identification of fib-1 were in fact raised against amniotic membrane from term placenta; moreover, the affinity purification of fibrillin was performed using fibroblast culture media (Sakai et al., 1986). Our data suggest that both of these sources contain little if any fib-2. In retrospect, however, indirect evidence for fibrillin heterogeneity can be found in the literature.

A few reports appeared in the early 70s suggesting the presence of microfibrils in elastic cartilage, where it is now known that there is little or no fib-1 deposition (Ishihara et al., 1973; Sanzone and Reith, 1976; Nielsen, 1976). Others, however, questioned these early findings of "peripheral elastin-associated" microfibrils in mature elastic cartilage (Serafini-Fracassini and Smith, 1974; Quintarelli et al., 1979; Kostovic-Knezevic et al., 1981). In particular, Quintarelli et al. (1979) argued that the elastic cartilage of the rabbit ear is formed by fusion of amorphous elastin into bundles of small filaments that are not seen at the periphery of mature elastic fibers. The same authors also found these fine filaments associated within the elastin purified from cultured chondrocytes. Kostovic-Knezevic et al. (1981) later confirmed the absence of microfibrils in the elastic core of the adult rat ear, but showed microfibrils in the periochondrium. Consistent with this finding, a review by Clearly and Gibson (1983) cited that polyclonal antibodies against a microfibrillar extract of bovine nuchal ligament failed to detect microfibrils in elastic cartilage. The authors attributed this failure to the masking of the epitopes by proteoglycans. Beside epitope masking, we believe that other major reasons for our delayed appreciation of microfibrillar structures in elastic cartilage were the specificity of the antibodies used and the age of the samples examined.

In all but one case, developmental expression of the fibrillin genes exhibits a characteristic diphasic pattern, with onset of *fbn2* transcription occurring earlier than *fbnl* expression. Consistent with the in situ data of Yin et al. (1995), the exception is the cardiovascular system, in which *fbnl* gene activity is early and always higher than *fbn2*. Although yet to be rigorously confirmed, in all other organ systems there is an apparent correlation between the time of expression of each fibrillin gene and distinct stages of morphogenesis. Accumulation of *fbn2* transcripts seems in fact to plateau just before overt tissue differentiation and to decrease rapidly or even disappear thereafter; in contrast, the amount of *fbnl* transcripts increases at an apparently gradual rate through-

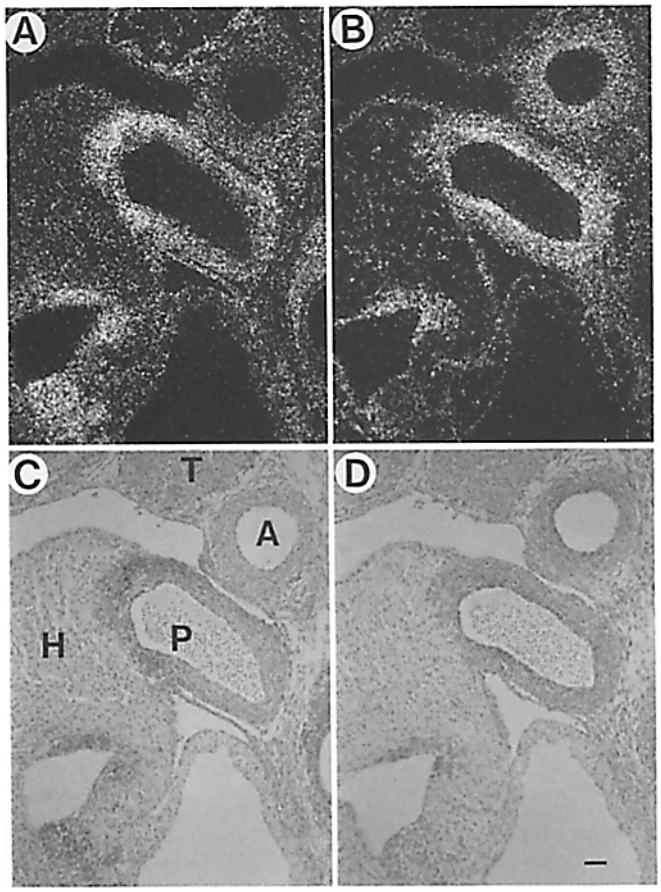

Figure 11. Expression of *fbn2* (*A* and *C*) and *fbnl* (*B* and *D*) in the heart (*H*) and elastic vessels of the 13.5-d.p.c. mouse. Both the intimal and medial cells of the pulmonary trunk (*P*) and aorta (*A*) have strong expression of *fbnl*, whereas the *fbn2* message is observed mostly in the medial layer, particularly its outer portion. The myocardial cells express the *fbn2* gene, thus giving a nearly uniform pattern of hybridization in the heart. In contrast, expression of the *fbnl* gene (most probably by the endothelial cells and fibroblasts of the cardiac skeleton) gives a somewhat punctate pattern. The capsule and the septa of the thymus (*T*) also show fibrillin expression. Bar, 50 μm.

out morphogenesis. The developing lung best exemplifies this point.

Elastogenesis in the lung is synchronized with the formation of primary, secondary, and tertiary bronchi and arterioles (Jones and Barson, 1971). Unlike *fbnl*, the *fbn2* gene is prominently expressed in bronchiolar epithelial cells and temporally restricted to the stages when either bronchi (10.5 and 13.5 d.p.c.) or bronchioles (16.5 d.p.c.) are developing. Although expressed throughout the lung mesenchyme and the smooth muscle cells of the bronchi, *fbnl* is inactive in the epithelium of the bronchiolar tree. Elastic tissue characterizes the airway of the lung; elastic fibers are in fact found in the lamina propria, submucosa, cartilaginous and muscular layers, and adventitia of the bronchial wall (Sorokin, 1988). Along these lines, Collert and Des Biens (1974) reported the finding of "microfilaments" located between the epithelial basal lamina and the underlying smooth muscle cells, as well as around the smooth muscle cells. The same authors also showed that both areas of the developing lung bronchi are sites of elastin deposition (Collert and Des Biens, 1974). A subsequent in situ hybridization analysis documented that the smooth muscle cells immediately adjacent to the epithelium of the newly formed bronchi are indeed the major sites of elastin production (Noguchi and Samaha, 1991). We believe our results support the idea that the microfilaments described in these early reports are made mostly of fib-2 and thus are biochemically distinct from those located in other parts of the lung. Interestingly, there is evidence for different enzymatic susceptibility of the microfibrils present in the lamina propria of the trachea (Bodley and Wood, 1971). This observation may reflect differences in either biochemical composition or physical accessibility of the microfibrils. The latter possibility implies that a specific kind of microfibril becomes buried within the elastic fiber. Such a conclusion is consonant with the aforementioned phenomenon of epitope masking in elastic cartilage, as well as with our own experience of reduced immunodetection of fib-2 in adult tissues compared with embryonic ones. Although we stress the phenomenologic correlation between *fbn2* gene expression and elastogenesis in tissues like lung and cartilage, we are also aware of important exceptions that point to a broader role of fibrillins in matrix function. For example, our analysis showed low levels of *fbn2* gene expression at several elastogenic sites, including the large vessels and arterioles, where there is significant fbn-1 deposition. We also saw substantial *fbn2* gene expression in tissues known to lack elastic fibers, such as the kidney. Hence our proposed function for each fibrillin should be considerd as a distinguishing attribute rather than an exclusive feature.

Microfibrils are generally believed to direct elastogenesis and to provide force-bearing structural support (Mecham and Davis, 1994). The former role is based on the observation that microfibrils appear first in the form of presumptive elastic fibers in developing elastic tissues and in vitro culture systems (Cleary and Gibson, 1983). The structural function can instead be inferred from the tissue distribution, pathology, and ultrastructural characteristics of the microfibrils (Ramirez et al., 1993; Rosenbloom et al., 1993). Based on the spatiotemporal patterns of gene expression, we suggest that each of the fibrillins plays predominantly, but not exclusively, one of these two roles. As already discussed, fib-2 is preferentially found in elastic tissues, such as the elastic cartilage, the tunica media layer of the aorta, and along the bronchial tree. During embryogenesis, fib-2 production begins earlier than fib-1 and is apparently limited to a window of time immediately preceding elastogenesis. We therefore argue that one of the major functions of fib-2 during early morphogenesis is to participate in directing elastic fiber assembly. Consistent with this prediction, microfibrils that are present during morphogenesis of the external ear are subsequently buried within elastin, thus leaving the mature structures without visible peripheral microfibrils (Sanzone and Reith, 1976; Serafini-Fracassini and Smith, 1974; Quintarelli et al., 1979). Both our immunohistochemical and our in situ data suggest that these microfibrils are made mostly of fib-2 (Zhang et al., 1994). The predominance of fib-1 in stress- and load-bearing structures—like aortic adventitia, suspensory ligament of the lens, and skin—suggests that this glycoprotein may be mostly responsible for the structural function of the microfibrils. Consistent with this conclusion,

the symptomatology of Marfan syndrome shows clinical signs of premature wearing-out of defective load-bearing structures, such as aortic aneurysm and ectopia lentis (Ramirez et al., 1993). Our finding that the only elastic tissue in a stress-free condition—the elastic cartilage—contains very little fib-1 protein lends further support to this hypothesis.

We believe that there is also some structural evidence for the postulated "regulatory" function of fib-2. We are referring to region C, the most divergent sequence of the fibrillins. We have previously proposed that region C may provide flexibility to the molecules, thus facilitating protein–protein interactions at the cysteine-rich regions (Pereira et al., 1993; Zhang et al., 1994). We now argue that these sequences may themselves participate in protein–protein interactions. In the case of fib-1, this prediction is in line with the recently established role of proline-rich peptides in promoting protein aggregation (reviewed by Williamson, 1994). The highly hydrophobic glycine-rich region of fib-2, on the other hand, shows homology with multiple segments of elastin (Rosenbloom et al., 1993). Like them, the glycine-rich region of fib-2 can theoretically form β-sheets or β-turns, promoting protein aggregation through interdigitation of the hydrophobic side chains (Robson et al., 1993). Thus, we postulate that region C of fib-2 may mediate critical interactions with elastin during the early assembly of elastic fibers. This is in turn consistent with the predominant or exclusive deposition of fib-2 at earlier stages of development in some of the matrices that will be eventually enriched in elastin.

In conclusion, this report demonstrates that the fibrillins are developmentally regulated genes with distinct spatiotemporal patterns. Based on evidence from this and our previous study (Zhang et al., 1993), we interpret the data as suggesting functional diversification of the extracellular microfibrils. The availability of the mouse fibrillin clones will enable us to test this hypothesis by introducing structural mutations in the fibrillin genes using the technique of homologous recombination in embryonic stem cells (Andrikopoulos et al., 1995).

The authors wish to thank Drs. J. Bonadio and S. Apfelroth for their generous support, T. Lufkin for the kind gift of the cDNA library, K. Andrikopoulos and D. Sasson for helpful advices, and Ms. M. Sozomenu for typing the manuscript. This is article 182 from the Brookdale Center for Molecular Biology.

Received for publication 19 December 1994 and in revised form 15 February 1995.

References

Andrikopoulos, K., H. R. Suzuki, M. Solursh, and F. Ramirez. 1992. Localization of pro-α2(V) collagen transcripts in the tissues of the developing mouse embryo. *Dev. Dyn.* 195:113–120.

Andrikopoulos, K., X. Liu, D. R. Keene, R. Jaenisch, and F. Ramirez. 1995. Targeted mutation in the *col5a2* gene reveals regulatory role of type V collagen during matrix assembly. *Nature Genet.* 92:31–36.

Bodley, D. H., and R. Wood. 1971. Ultrastructural studies on elastic fibers using enzymatic digestion of thin sections. *Anat. Rec.* 172:71–88.

Cleary, E. G., and M. A. Gibson. 1983. Elastin-associated microfibrils and microfibrillar proteins. *Int. Rev. Connect. Tissue Res.* 10:97–209.

Collert, A. J., and G. Des Biens. 1974. Fine structure of myogenesis and elastogenesis in the developing rat lung. *Anat. Rec.* 179:343–360.

Corson, G. M., S. C. Chalberg, H. C. Dietz, N. L. Charbonneau, and L. Sakai. 1993. Fibrillin binds calcium and is coded by cDNAs that reveal a multidomain structure and alternatively spliced exons at the 5′ end. *Genomics.* 7:476–484.

Dietz, H. C., G. R. Cutting, R. E. Pyeritz, C. Maslen, L. Y. Sakai, G. M. Corson, E. G. Puffenberger, A. Hamosh, E. J. Nantakumar, S. M. Curristin, G. Stetten, D. A. Meyers, and C. A. Francomano. 1991. Marfan syndrome caused by a recurrent *de novo* missense mutation in the fibrillin gene. *Nature (Lond.).* 352:337–339.

Gibson, M. A., L. B. Sandberg, L. E. Grosso, and E. G. Cleary. 1991. Complementary DNA cloning establishes microfibril-associated glycoprotein (MAGP) to be a discrete component of elastin-associated microfibrils. *J. Biol. Chem.* 264:4590–4598.

Horrigan, S. K., C. B. Rich, B. W. Streeten, Z. Y. Li, and J. A. Foster. 1992. Characterization of an associated microfibril protein through recombinant DNA techniques. *J. Biol. Chem.* 267:10087–10095.

Ishihara, T., T. Iwata, F. Furutani, F. Uchino, S. Maeda, G. Mogu, and S. Honjo. 1973. Relapsing polycondritis--report of a case with ultrastructural findings of the ear cartilage. *Acta Pathol. Japan.* 23:577–590.

Jones, A. W., and A. J. Barson. 1971. Elastogenesis in the developing chick lung: a light and electron microscopical study. *J. Anat.* 110:1–15.

Kaufman, M. H. 1992. The Atlas of Mouse Development. Academic Press, Inc., San Diego, CA. 512 pp.

Kawasaki, E. S., and A. M. Wang. 1989. Detection of gene expression. *In* PCR Technology: Principles and Applications for DNA Amplification. H. A. Erlich, editor. Stockon Press, New York. 89–98.

Kostovic-Knezevic, L., Z. Bradamante, and A. Svajger. 1981. Ultrastructure of elastic cartilage in rat external ear. *Cell Tissue Res.* 218:149–160.

Lee, B., M. Godfrey, E. Vitale, H. Hori, M. G. Mattei, M. Sarfarazi, P. Tsipouras, F. Ramirez, and D. W. Hollister. 1991. Linkage of Marfan syndrome and a phenotypically related disorder to two fibrillin genes. *Nature (Lond.).* 352:330–334.

Li, X., L. Pereira, H. Zhang, C. Sanguineti, F. Ramirez, J. Bonadio, and U. Francke. 1993. Fibrillin genes map to regions of conserved mouse/human synteny on mouse chromosomes 2 and 18. *Genomics.* 18:667–672.

Maslen, C. L., G. M. Corson, B. K. Maddox, R. W. Glanville, and L. Y. Sakai. 1991. Partial sequence of a candidate gene for the Marfan syndrome. *Nature (Lond.).* 352:334–337.

Mecham, R. P., and E. C. Davis. 1994. Elastic fiber structure and assembly. *In* Extracellular Matrix Assembly and Structure. P. D. Yurchenco, D. E. Birk, and R. P. Mecham, editors. Academic Press, Inc., New York. 281–314.

Nielsen, E. H. 1976. The elastic cartilage in the normal rat epiglottis. *Cell Tissue Res.* 173:179–191.

Noguchi, A., and H. Samaha. 1991. Developmental changes in tropoelastin gene expression in the rat lung studied by *in situ* hybridization. *Am. J. Respir. Cell Mol. Biol.* 5:571–578.

Pereira, L., M. D'Alessio, F. Ramirez, J. R. Lynch, B. Sykes, T. Pangilinam, and J. Bonadio. 1993. Genomic organization of the sequence coding for fibrillin, the defective gene product in Marfan syndrome. *Hum. Mol. Genet.* 2:961–968.

Quintarelli, G., B. C. Starcher, A. Vacaturo, F. di Gianfilippo, L. Gotte, and R. P. Mecham. 1979. Fibrogenesis and biosynthesis of elastin in cartilage. *Connect. Tissue Res.* 7:1–19.

Ramirez, F., L. Pereira, H. Zhang, and B. Lee. 1993. The fibrillin–Marfan syndrome connection. *BioEssays.* 15:589–594.

Robson, P., G. M. Wright, E. Sitarz, A. Maiti, M. Rawat, J. H. Younson, and F. W. Keeley. 1993. Characterization of lamprin, an unusual matrix protein from lamprey cartilage. *J. Biol. Chem.* 268:1440–1447.

Rosenbloom, J., W. R. Abrams, and R. P. Mecham. 1993. Extracellular matrix 4: the elastic fiber. *FASEB (Fed. Am. Soc. Exp. Biol.) J.* 7:1208–1218.

Sakai, L. Y., D. R. Keene, and E. Engvall. 1986. Fibrillin, a new 350-kD glycoprotein, is a component of connective tissue microfibrils. *J. Cell Biol.* 103:2499–2509.

Sakai, L. Y., D. R. Keene, R. W. Glanville, and H. P. Bächinger. 1991. Purification and partial characterization of fibrillin, a cysteine-rich structural component of connective tissue microfibrils. *J. Biol. Chem.* 266:14763–14770.

Sambrook, J., E. F. Fritsch, and T. Maniatis. 1989. Molecular Cloning: A Laboratory Manual. Second edition. Cold Spring Harbor Laboratory Press, Cold Spring Harbor, NY. 545 pp.

Sanzone, C. F., and E. J. Reith. 1976. The development of the elastic cartilage of the mouse pinna. *Am. J. Anat.* 146:31–72.

Serafini-Fracassini, A., and J. W. Smith. 1974. The Structure and Biochemistry of Cartilage. Churchill-Livingstone, London. 228 pp.

Sorokin, S. P. 1988. The respiratory system. *In* Cell and Tissue Biology. L Weiss, editor. Urban and Schwarzenberg Inc., Baltimore, MD. 753–814 pp.

Su, M. W., H. R. Suzuki, J. J. Bieker, M. Solursh, and F. Ramirez. 1991. Expression of two nonallelic type II procollagen genes during *Xenopus laevis* embryogenesis is characterized by stage-specific production of alternatively spliced transcripts. *J. Cell Biol.* 115:565–575.

Williamson, M. P. 1994. The structure and function of proline-rich regions in proteins. *Biochem. J.* 297:249–260.

Yin, W., E. Smiley, J. Germiler, C. Sanguineti, T. Lawton, L. Pereira, F. Ramirez, and J. Bonadio. 1995. Primary structure and developmental expression of *Fbn-1*, the mouse fibrillin gene. *J. Biol. Chem.* 270:1798–1806.

Zagursky, R. J., M. L. Berman, K. Baumister, and N. Lomax. 1986. Rapid and easy sequencing of linear double stranded DNA and supercoiled plasmid DNA. *Gene Anal. Tech.* 2:89–94.

Zhang, H., D. S. Apfelroth, W. Hu, E. C. Davis, C. Sanguineti, J. Bonadio, R. P. Mecham, and F. Ramirez. 1994. Structure and expression of fibrillin-2, a novel microfibrillar component preferentially located in elastic matrices. *J. Cell Biol.* 124:855–863.